

Enhancing the Reactivity of Al/CuO Nanolaminates by Cu Incorporation at the Interfaces

Lorena Marín,^{†,⊥} Charith E. Nanayakkara,[#] Jean-Francois Veyan,[#] Bénédicte Warot-Fonrose,^{‡,⊥} Sébastien Joulie,^{‡,⊥} Alain Estève,^{†,⊥} Christophe Tenailleau,^{§,⊥} Yves J. Chabal,[#] and Carole Rossi^{*,†,⊥}

[†]LAAS-CNRS, 7 Avenue du colonel Roche, F-31077 Toulouse, France

[‡]CEMES-CNRS, 29, Rue Jeanne Marvig, F-31055 Toulouse, France

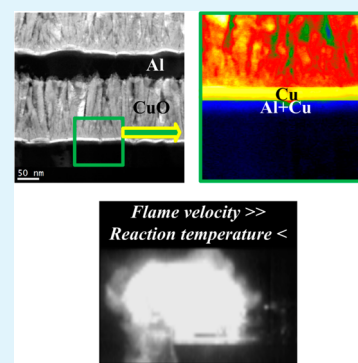
[§]CIRIMAT-CNRS, 118 Route de Narbonne, F-31062 Toulouse Cedex 9, France

[⊥]UPS, INSA, INP, ISAE, LAAS, Université de Toulouse, F-31062 Toulouse, France

[#]Department of Materials Science and Engineering, The University of Texas at Dallas, Richardson, Texas 75080, United States

Supporting Information

ABSTRACT: In situ deposition of a thin (~5 nm) layer of copper between Al and CuO layers is shown to increase the overall nanolaminate material reactivity. A combination of transmission electron microscopy imaging, in situ infrared spectroscopy, low energy ion scattering measurements, and first-principles calculations reveals that copper spontaneously diffuses into aluminum layers (substantially less in CuO layers). The formation of an interfacial Al:Cu alloy with melting temperature lower than pure Al metal is responsible for the enhanced reactivity, opening a route to controlling the stoichiometry of the aluminum layer and increasing the reactivity of the nanoenergetic multilayer systems in general.



KEYWORDS: nanothermite, CuO, Al, Cu, Cu enriched multilayers, intermixing, nanoenergetic materials

Recent advances in integrating reactive materials into semiconducting electronic structures have opened up the era of “nanoenergetics-on-a-chip” technology, which has a wide range of potential applications, such as micropropulsion in space and nanoairbags to drive fluids, MEMS energy sources,¹ pressure-mediated molecular delivery,^{2,3} and microinitiators.^{4,5} Currently, nanothermites composed of metal and oxide microstructures are the most widely used energetic materials for device integration. These materials are characterized by high-energy release associated with the highly exothermic reduction/oxidation reactions in forming suboxides.

Thermite multilayered systems are promising structures for integrating energetic layers on a chip because it is easy to control the thickness of each layer and the number of layers, and consequently to tune their energetic performances. In the present work, we select Al/CuO thin film multilayer systems (also called nanolaminates) because they are characterized by much higher reaction velocity than other multilayer systems such as Al/Ni systems.⁶ Al/CuO multilayers with different bilayer (Al+CuO) thicknesses have been sputter-deposited on solid surfaces^{7–11} and their properties analyzed experimentally and theoretically. Measurements of the flame propagation velocity versus the bilayer thickness in stoichiometric mass ratio show that the reaction-propagation velocity decreases from 90 to 2 m/s as the foils thickness increases from 50 to 2000 nm.

However, if the bilayer thickness is further decreased below 25 nm, the velocity drops rapidly to zero due to spontaneous and uncontrolled intermixing at the interface during deposition (see the Supporting Information, Figure S1a). This finding highlights the critical role of the interfacial region on the reaction kinetics.¹² Namely, the flame propagation velocity increases with decreasing bilayer thickness only if the latter remains substantially larger than the interfacial region thickness.

The goal of this experimental work is to find technological solutions to enhance Al/CuO multilayer system reactivity without penalizing its safety or stability at low temperature. We find that depositing a thin layer of copper (~5 nm in thickness) on each ~100 nm thick Al layer prior to the deposition of ~200 nm thick CuO layers substantially increases the overall Al/CuO nanolaminate flame propagation velocity and also lowers the onset temperature. The measured flame velocity increases to 72 ± 1 m/s with copper-enriched Al/CuO nanolaminates, compared to 44 ± 1 m/s for the Al/CuO nanolaminates prepared by conventional Al and CuO deposition. Furthermore, combining transmission electron microscopy (TEM), infrared spectroscopy (IR), X-ray photoelectron spectroscopy (XPS), low energy ion

Received: March 26, 2015

Accepted: May 19, 2015

Published: May 19, 2015

scattering (LEIS), and differential scanning calorimetry (DSC) measurements with first-principles calculations, we show that Cu deposition leads to the formation of an Al:Cu alloy characterized by a melting temperature lower than that of pure Al metal. DSC analysis indicates that the Al:Cu alloy melting point is 110 °C lower than the Al melting point, which is consistent with the observed increase in the overall reactivity.

Three different foils were prepared to perform a head-to-head comparison: (a) Al/Cu/CuO/Cu/Al (i.e., a trilayer with Cu in both interfaces); (b) seven Al/CuO bilayers (i.e., without any Cu deposition in between); and (c) seven Al/Cu/CuO trilayers called Cu-enriched Al/CuO nanolaminates. In all samples, the thicknesses of the Al, CuO, and Cu layers were around 100, 200, and 5 nm, respectively, and were deposited using magnetron sputtering as previously described⁸ (see more details in the Supporting Information, Figure S1b). The exothermic reactions of Al/CuO nanolaminates were characterized by DSC in the temperature range of 30 to 700 °C under constant heating rate (10 °C/min) and under Ar atmosphere. The self-propagating reaction velocity was measured by placing the free-standing foils in an open elongated channel, directly igniting one end with a metallic wire and optically measuring the propagation of the flame using a high-speed camera.

All foils release heat upon heating, as observed by DSC trace (see Figure 1) with a major exothermic peak rising abruptly.

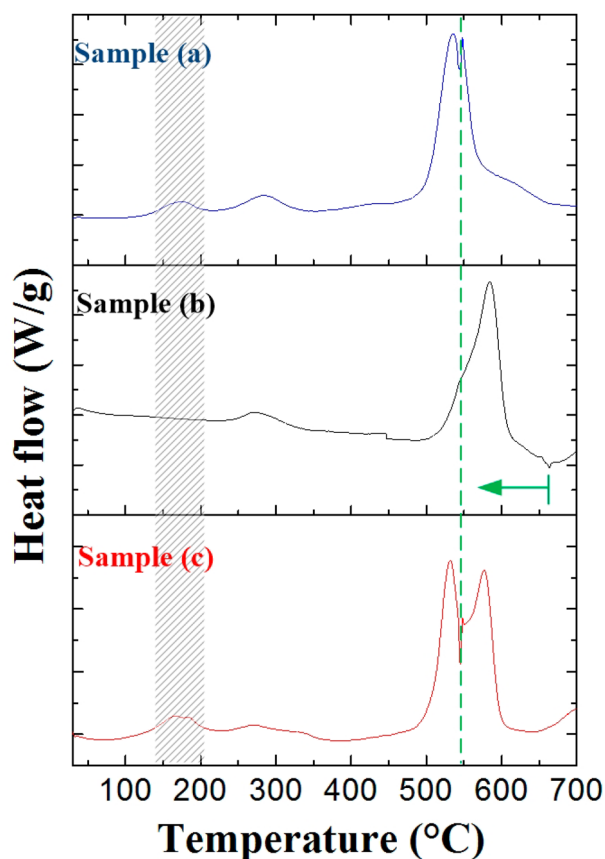


Figure 1. DSC curves of Al/CuO as a function of the temperature in Ar environment: (a) Al/Cu/CuO/Cu/Al; (b) seven Al/CuO bilayers; and (c) seven Al/Cu/CuO trilayers. The curves have been normalized to the mass value. Two remarkable features of the DSC curves are highlighted in the figure, one around 175 °C certainly corresponding to Cu:Al alloying and a second one showing the shift of melting point from 660 to 548 °C.

The heats of reaction calculated through the integration of the major peak is 1.2 ± 0.3 , 1.0 ± 0.3 , and 1.3 ± 0.3 kJ/g for samples a, b, and c, respectively. Note that the heats are well below maximum values, around 33% of theoretical ones, because the reactions are incomplete below 700 °C. But still, differences are noticeable. Without copper between Al and CuO (sample b), the main exothermic peak is observed at 584 °C and the onset is at around 550 °C. In contrast, the incorporation of copper (sample a and c) induces a reduction of the onset temperature (~ 475 °C) and reaction temperature (535 and 532 °C, respectively). In addition, for Cu-enriched Al/CuO nanolaminates and for the trilayers with Cu at both interfaces, two small exotherms occur at 175 and 275 °C, suggesting Cu:Al alloy formation,¹³ and a shift of melting point is also observed from 660 to 548 °C.

Both bright-field TEM and scanning TEM (STEM) images reveal that the interfaces between sputter deposited aluminum and copper oxide for samples a and c are sharp and well-defined as show in Figure 2a, c, whether there is the extra 5 nm thick Cu layer or not at the interface. Nanoscale chemical analysis was performed using Energy-dispersive X-ray (EDX) spectroscopy on sample a, clearly showing (Figure 2b) Cu atoms dispersed in Al layer and indicating that there is spontaneous intermixing of Cu and Al. In fact, there is more Cu inside (at the center) of the Al films than in the thin interfacial region where the Cu was deposited, suggesting a strong drive for Cu to diffuse deep into Al. (more detail is given in the Supporting Information, Figure S3, top). Sample c was analyzed using STEM mode by high-angle annular dark field (HAADF) and electron energy-loss spectroscopy (EELS). The EELS fine structures are sensitive to the chemical environment of the studied atom. The signature of metallic Cu is different from a Cu atom surrounded by O in CuO (see the Supporting Information, Figure S3, Bottom). In Figure 2d, we can see some Cu signal in the same spectra of the Al, clearly showing the intermixing of Al and Cu, which is in good agreement with experiments obtained by a model study in a cluster tool (in ultrahigh vacuum) with in situ XPS, FTIR, LEIS supported by DFT (density functional theory) calculations. First, 5 nm of Cu was e-beam deposited on CuO (5.4 Å/min) in high vacuum (1×10^{-9} Torr) at 10 °C. The broadband in situ IR absorption (see the Supporting Information, Figure S4) confirms the formation of a metallic layer (Drude absorption). The spectra also indicate that the surface is highly inhomogeneous surface, because of the fact that CuO is formed of pillars with a rough surface, leading to nonuniform Cu deposition. In addition, there is some reduction of CuO into Cu₂O after 5 nm Cu deposition, as evidenced by the appearance of a Cu₂O phonon peak at 620 cm⁻¹, which is consistent with some Cu incorporation into CuO. In contrast, Cu deposition on Al leads to additional broadband IR absorption, which suggests that the pure Al film was altered, consistent with Cu migration into Al.

LEIS is most appropriate to determine the surface composition. Figure 3a summarizes the main LEIS spectra obtained at room temperature after Cu deposition on CuO at 10 °C and as a function of annealing up to 200 °C. The bottom LEIS spectrum (black) in Figure 3a is for the CuO before any deposition. The Cu and O features are both present, although weak because of surface contamination. After 5 nm Cu deposition, the Cu signal is significantly increased, with a relatively weak O signal, as shown in the red spectrum. The top two spectra, obtained after annealing to 150 and 200 °C, show a constant Cu:O ratio, although both signals increase because of removal of all contamination.

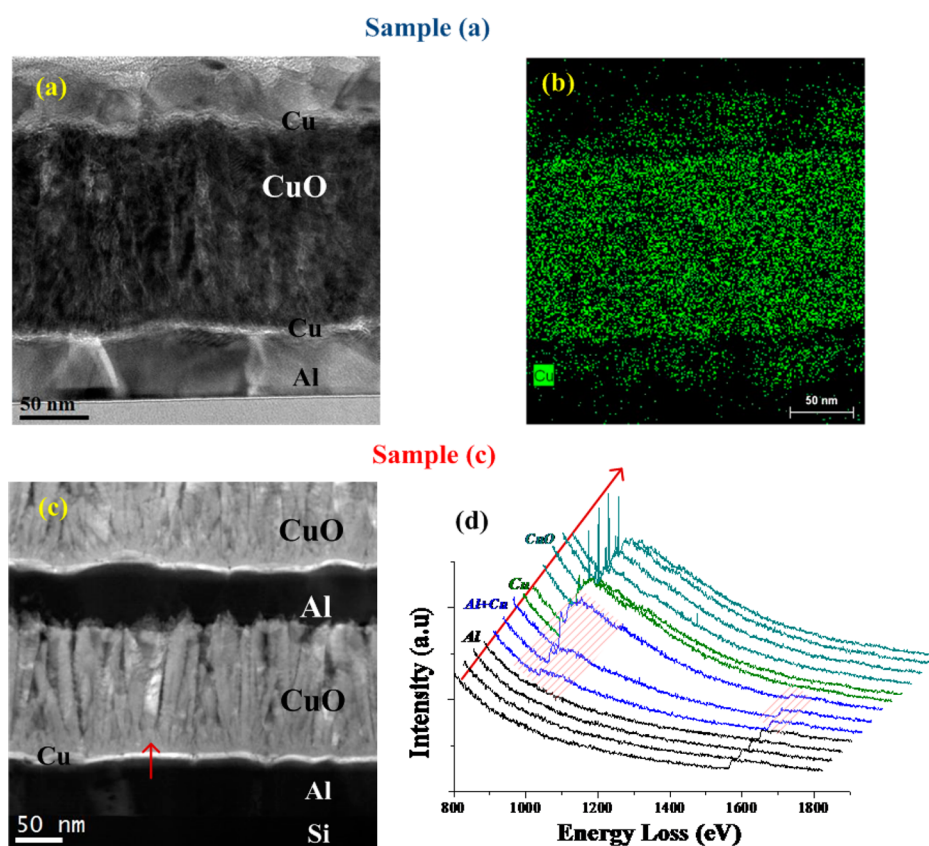


Figure 2. (a) Bright-field TEM image and (b) EDX spectroscopy to repartition of Cu across of the sample (a); (c) STEM image; and (d) EELS spectra for Cu and Al across the Al/Cu/CuO interface (red arrow).

These results suggest that the surface chemical composition remains unchanged, i.e. there is not a strong drive for Cu to diffuse into CuO.

The situation is different for Cu deposited on Al films. To explore this situation, a thin single-crystal Al (111) film is first deposited by evaporating at a rate of 4.4 Å/min on a H-terminated Si (111) surface at -140 ± 5 °C, according to a method previously described by Liu et al.¹⁴ IR transmission experiments confirm that a good metallic film is formed (strong Drude absorption). LEIS spectra collected after Al deposition confirm the presence of the Al at the topmost layer together with a small amount of a surface aluminum oxide, probably formed during the transfer from the deposition chamber to the LEIS chamber despite UHV conditions (see the Supporting Information, Figure S5). For 1 nm Cu deposition at room temperature (as measured with a QCM) on a 10 nm thick Al film, no Cu is detected (see Figure 3b), indicating full penetration into Al at room temperature. Therefore, a higher Cu dose was used on a substrate at lower temperature -140 ± 5 °C. After 5 nm Cu deposition on a 20 nm thick Al film, the topmost layer atomic composition determined by LEIS (bottom spectrum in Figure 3c does now have a substantial amount of Cu (Cu:Al ratio = 46) even though the measurements are performed at room temperature. A small amount of O and Al suggest that the Cu layer is either thin or inhomogeneous. Upon annealing to 150 °C, the Cu:Al ratio decreases dramatically (Cu:Al ratio = 0.7), consistent with Cu incorporation in the Al film. Further annealing to 200 °C does not significantly change the Al and Cu signals (Cu:Al ratio ~ 0.5), suggesting that the surface composition is now in equilibrium with a Cu:Al alloy in the bulk (i.e., the near-surface region has reached a stable stoichiometry).

To examine the chemical composition deeper into the Al layer, XPS experiments were performed. Figure 4a shows the changes in the Cu 2p core level of CuO before and after 5 nm Cu deposition. The data clearly shows the reduced Cu with the peak at 932.4 eV, although it is difficult to distinguish Cu₂O and metallic Cu from the XPS due to the overlapping of peaks originating from the two species. Figures 4b, c contain the Cu 2p and Al 2p core level spectra after 5 nm Cu deposited on 20 nm Al (at -140 °C) and after annealing to 200 °C. In Figure 4b, the peak position of Cu (933.6 eV) is very close to that observed in Al₂Cu (933.8 eV),¹⁵ clearly indicating the formation of such an alloy. The data in the 74–84 eV range in Figure 4c includes both the Al 2p and Cu 3p core levels, with a splitting between metallic and oxidized aluminum. This result is in agreement with our recent DFT calculations¹⁶ that described the energetics of copper penetration into Al (111) through surface exchange mechanisms involving energy gains of ~ 0.1 eV and barriers of ≤ 0.5 eV, indicating that penetration of incident copper atoms will take place at ambient temperature at the initial stage of copper deposition.

Combining all the TEM, IR, EDX, EELS, XPS, and LEIS data, we conclude that Cu penetrates spontaneously into the Al layer, a prerequisite for alloy formation. The weak exothermic peak in the DSC at 175 °C suggests that the formation of stoichiometric and stable alloys, Cu₉Al₄ and CuAl₂ does require some thermal activation.

Similarly, DFT calculations of Cu interaction with CuO surface reveal that adsorption is favorable, mostly on the O sites of oxygen-rich CuO surfaces (2.63 eV adsorption energy). However, penetration is endothermic by +1.2 eV, i.e., unfavorable. The observation of Cu₂O in the IR spectra indicate that energetic Cu atoms can penetrate to a limited extent, but lead

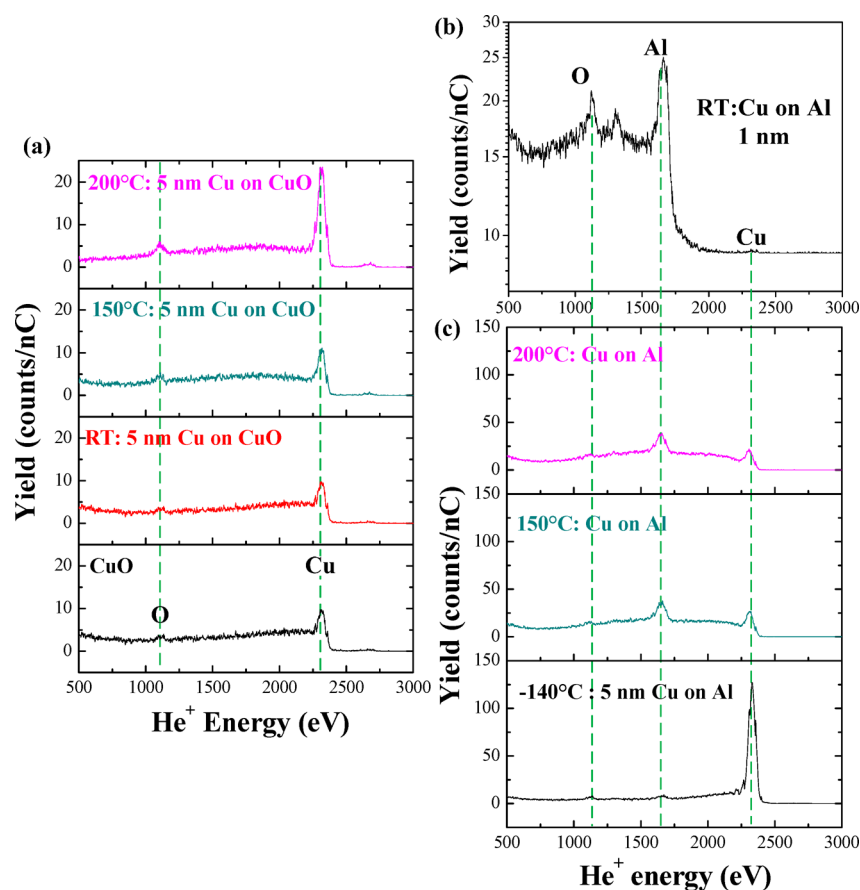


Figure 3. LEIS spectra (all measured at room temperature) of (a) CuO substrates before and after 5 nm Cu deposition at room temperature (RT) and subsequent annealing to 150 and 200 °C, (b) 10 nm Al films after 1 nm Cu deposition at room temperature (RT), and (c) 20 nm Al films after 5 nm Cu on Al at -140 °C and subsequent annealing to 150 and 200 °C.

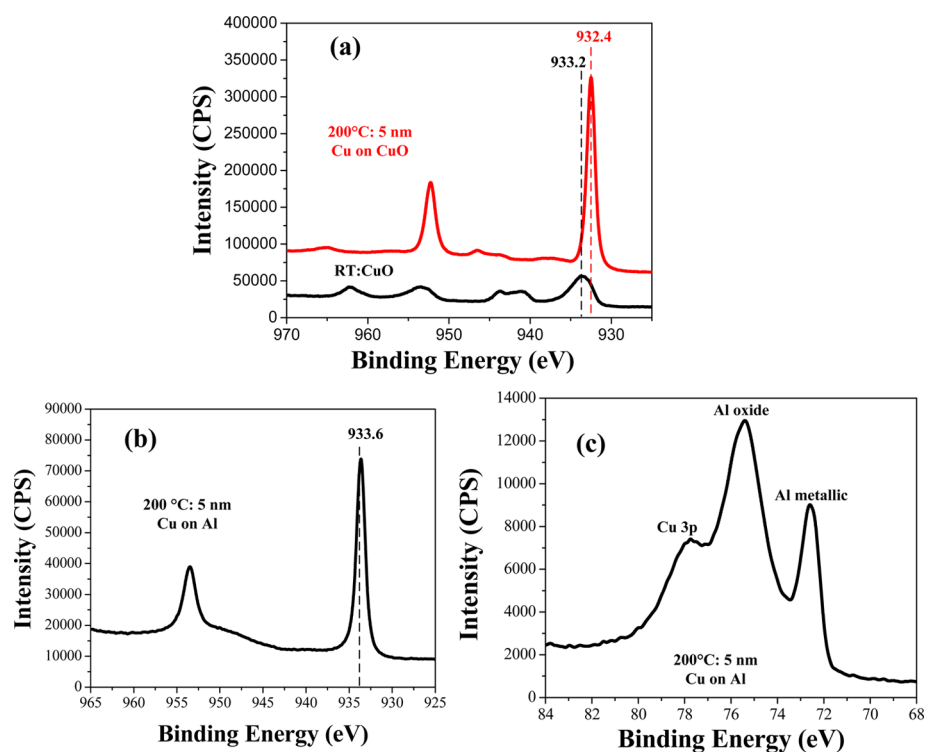


Figure 4. (a) Cu 2p core level spectra from CuO and after 5 nm Cu deposition (at 10 °C) and annealing to 200 °C, (b) Cu 2p core level spectra from 5 nm Cu deposition (at -140 °C) on Al and after annealing to 200 °C, and (c) Al 2p core level spectra from 5 nm Cu deposition (at -140 °C) on Al and after annealing to 200 °C.

to a defective surface. Details regarding this point are given in the Supporting Information, Figure S6.

The limited penetration of Cu into CuO is also consistent with DSC experiments of foils made of 7 bilayers of aluminum and copper-rich copper oxide (Cu_xO_y , such Cu_4O_3 , Cu_2O), keeping the same Al and Copper oxide thickness (~ 100 and 200 nm, respectively). As shown in Table 1, summarizing the

Table 1. Average Self-Propagating Flame Velocity As a Function of CuO Stoichiometry (All Al/CuO_x Foils Were of ~ 2 μm as Total Thickness)

composition of the bilayers	Al/CuO	Al/Cu ₂ O	Al/Cu ₄ O ₃	Al/Cu _x O _y ^a	Al/Cu/CuO
self-propagation rate (m/s ± 1)	44	22	18	5	72
heat of reaction (kJ/g ± 0.3)	1.0	0.8	1.0	0.9	1.3

^aThis nomenclature represents the mix phase $\text{Cu}_2\text{O}-\text{Cu}_4\text{O}_3-\text{CuO}$

effect of CuO_x stoichiometry on thermal reaction properties, there is a dramatic decrease in the reaction propagation velocity with Cu enrichment of copper oxide down to 5 m/s when for an oxide composed of a $\text{Cu}_2\text{O}/\text{Cu}_4\text{O}_3/\text{CuO}$ mixture. Therefore, a similar loss in flame propagation velocity would also be expected for the Al/Cu/CuO stack if Cu did penetrate into CuO and transformed its composition into Cu-rich oxide. This observation is an indirect proof that Cu incorporation into CuO during either sputter deposition or evaporation is at most limited to the CuO surface without modification of the overall 200 nm CuO layer stoichiometry.

In summary, we have shown that deposition of a thin (~ 5 nm) layer of Cu between each Al and CuO layers of an Al/CuO nanolaminate greatly enhances the system reactivity by Cu diffusion into Al and formation of Cu:Al alloys, which lowers the metallic melting temperature of the reducer (Al) and therefore increases the reaction propagation velocity. Both LEIS and XPS suggest that Cu penetrates deeply into Al films, while Cu only affects the surface region of CuO films. DSC indicates that stoichiometric and low-melting-temperature Al:Cu alloys are formed at relatively low temperatures (~ 175 °C)¹³ such as CuAl_2 or Cu_9Al_4 . The endotherm observed at 548 °C corresponds to the dissolution of these alloys into the Al solid solution leaving this latter phase in equilibrium with the liquid phase, which is consistent with an increase of the average self-propagating reaction velocity. These preliminary insights on the chemistry of interfaces generated upon Cu deposition pulses between Al and CuO open a new direction toward interface engineering of nanoenergetic materials and cautions against simplistic pictures of passive coating layers in application where the thermal and mechanical properties of metals are critical.

■ ASSOCIATED CONTENT

Supporting Information

Experimental details (sample preparation, TEM sample preparation, and experiments (TEM, XPS, LEIS, IR, EELS) spectra) are reported. The Supporting Information is available free of charge on the ACS Publications website at DOI: 10.1021/acsami.5b02653.

■ AUTHOR INFORMATION

Corresponding Author

*E-mail: carole.rossi@laas.fr.

Author Contributions

The manuscript was written through contributions of all authors. All authors have given approval to the final version of the manuscript.

Funding

This study is supported by ANR grant (CIREN 411531), NSF-DMR (1312525), and CNRS-INSIS (LIA-ATLAB).

Notes

The authors declare no competing financial interest.

■ ACKNOWLEDGMENTS

The authors thank the French Technological Network RENATECH having partially funded the sputter deposition equipment as well as CALMIP-1033 for computational resources and the French CNRS for the financial support of the METSA network (FR3507). We also thank Pierre Alphonse from CIRIMAT who assists us in the DSC experiments and Stéphane Pinon from LAAS for your valuable experimental work and assistance.

■ REFERENCES

- Rossi, C.; Zhang, K.; Estève, D.; Alphonse, P.; Tailhades, P.; Vahlas, C. Nanoenergetic Materials for MEMS: A Review. *J. Microelectromechanical Syst.* **2007**, *16*, 919–931.
- Ardila Rodríguez, G. A.; Suhard, S.; Rossi, C.; Estève, D.; Fau, P.; Sabo-Etienne, S.; Mingotaud, A. F.; Mauzac, M.; Chaudret, B. A Microactuator Based on the Decomposition of an Energetic Material for Disposable Lab-on-Chip Applications: Fabrication and Test. *J. Micromech. Microeng.* **2008**, *19*, 015006.
- Korampally, M.; Apperson, S. J.; Staley, C. S.; Castorena, J. A.; Thiruvengadathan, R.; Gangopadhyay, K.; Mohan, R. R.; Ghosh, A.; Polo-Parada, L.; Gangopadhyay, S. Transient Pressure Mediated Intranuclear Delivery of FITC-Dextran into Chicken Cardiomyocytes by MEMS-based Nanothermite Reaction Actuator. *Sensors Actuators B* **2012**, *171–172*, 1292–1296.
- Zhang, K.; Rossi, C.; Petrantoni, M.; Maura, N. A Nano Initiator Realized by Integrating Al/CuO-based Nanoenergetic Materials with a Au/Pt/Cr Microheater. *J. Microelectromech. Syst.* **2008**, *17*, 832–836.
- Taton, G.; Lagrange, D.; Conedera, V.; Renaud, L.; Rossi, C. Micro-chip Initiator Realized by Integrating Al/CuO Multilayer Nanothermite on Polymeric Membrane. *J. Micromech. Microeng.* **2013**, *23*, 105009.
- Knepper, R.; Snyder, M. R.; Fritz, G.; Fisher, K.; Knio, O. M.; Weihs, T. P. Effect of Varying Bilayer Spacing Distribution on Reaction Heat and Velocity in Reactive Al/Ni Multilayers. *J. Appl. Phys.* **2009**, *114*, 223517.
- Zhu, P.; Shen, R.; Ye, Y.; Fu, S.; Li, D. Characterization of Al/CuO Nanoenergetic Multilayer Films Integrated with Semiconductor Bridge for Initiator Applications. *J. Appl. Phys.* **2013**, *113*, 014901.
- Bahrami, M.; Taton, G.; Conédéra, V.; Salvagnac, L.; Tenailleau, C.; Alphonse, P.; Rossi, R. Magnetron Sputtered Al-CuO Nanolaminates: Effect of Stoichiometry and Layers Thickness on Energy Release and Burning Rate. *Propellants, Explos. Pyrotech.* **2014**, *39*, 365–373.
- Petrantoni, M.; Rossi, C.; Salvagnac, L.; Conédéra, V.; Estève, A.; Tenailleau, C.; Alphonse, P.; Chabal, Y. J. Multilayered Al/CuO Thermite Formation by Reactive Magnetron Sputtering: Nano versus Micro. *J. Appl. Phys.* **2010**, *108*, 1–6.
- Zhou, X.; Shen, R.; Ye, Y.; Zhu, P.; Hu, Y.; Wu, L. Influence of Al/CuO Reactive Multilayer Films Additives on Exploding Foil Initiator. *J. Appl. Phys.* **2011**, *110*, 094505.
- Manesh, N. A.; Basu, S.; Kumar, R. Experimental Flame Speed in Multi-Layered Nano-Energetic materials. *Combust. Flame* **2010**, *157*, 476–480.
- Kwon, J.; Ducéré, J. M.; Alphonse, P.; Bahrami, M.; Petrantoni, M.; Veyan, J. F.; Tenailleau, C.; Estève, A.; Rossi, C.; Chabal, Y. J.

Interfacial chemistry in Al/CuO reactive nanomaterial and its role in exothermic reaction. *ACS Appl. Mater. Interfaces*. **2013**, *5*, 605–613.

(13) Zschech, E.; Rennert, P. Phase shifts in the EXAFS of crystalline iron—experimental results and theoretical calculations. *Nucl. Instrum. Methods Phys. Res.* **1989**, *282*, 658–663.

(14) Liu, H.; Zhang, Y. F.; Wang, D. Y.; Pan, M. H.; Jia, J. F.; Xue, Q. K. Two-dimensional growth of Al films on Si(111)-7 × 7 at low-temperature. *Surf. Sci.* **2004**, *51*, 5–11.

(15) Liu, Y.; Bailey, P.; Noakes, T. C. Q.; Thompson, G. E.; Skeleton, P.; Alexander, M. R. Chemical environment of copper at the surface of a CuAl₂ model alloy: XPS, MEIS and TEM analyses. *Surf. Interface Anal.* **2004**, *36*, 339–346.

(16) Lanthony, C.; Guiltat, M.; Ducéré, J. M.; Verdier, A.; Hémercyck, A.; Djafari-Rouhani, M.; Rossi, C.; Chabal, Y. J.; Estève, A. Elementary Surface Chemistry during CuO/Al Nanolaminate- Thermite Synthesis: Copper and Oxygen Deposition on Aluminum (111) Surfaces. *ACS Appl. Mater. Interfaces*. **2014**, *111*, 15086–15097.